

Lecture Notes in Civil Engineering

Phung Duc Long
Nguyen Tien Dung *Editors*

Proceedings of the 5th International Conference on Geotechnics for Sustainable Infrastructure Development

GEOTEC2023; 14–15 Dec; Hanoi, Vietnam

 Springer

Lecture Notes in Civil Engineering

Volume 395

Series Editors

Marco di Prisco, Politecnico di Milano, Milano, Italy

Sheng-Hong Chen, School of Water Resources and Hydropower Engineering,
Wuhan University, Wuhan, China

Ioannis Vayas, Institute of Steel Structures, National Technical University of
Athens, Athens, Greece

Sanjay Kumar Shukla, School of Engineering, Edith Cowan University, Joondalup,
WA, Australia

Anuj Sharma, Iowa State University, Ames, IA, USA

Nagesh Kumar, Department of Civil Engineering, Indian Institute of Science
Bangalore, Bengaluru, Karnataka, India

Chien Ming Wang, School of Civil Engineering, The University of Queensland,
Brisbane, QLD, Australia

Zhen-Dong Cui, China University of Mining and Technology, Xuzhou, China

Lecture Notes in Civil Engineering (LNCE) publishes the latest developments in Civil Engineering—quickly, informally and in top quality. Though original research reported in proceedings and post-proceedings represents the core of LNCE, edited volumes of exceptionally high quality and interest may also be considered for publication. Volumes published in LNCE embrace all aspects and subfields of, as well as new challenges in, Civil Engineering. Topics in the series include:

- Construction and Structural Mechanics
- Building Materials
- Concrete, Steel and Timber Structures
- Geotechnical Engineering
- Earthquake Engineering
- Coastal Engineering
- Ocean and Offshore Engineering; Ships and Floating Structures
- Hydraulics, Hydrology and Water Resources Engineering
- Environmental Engineering and Sustainability
- Structural Health and Monitoring
- Surveying and Geographical Information Systems
- Indoor Environments
- Transportation and Traffic
- Risk Analysis
- Safety and Security

To submit a proposal or request further information, please contact the appropriate Springer Editor:

- Pierpaolo Riva at pierpaolo.riva@springer.com (Europe and Americas);
- Swati Meherishi at swati.meherishi@springer.com (Asia—except China, Australia, and New Zealand);
- Wayne Hu at wayne.hu@springer.com (China).

All books in the series now indexed by Scopus and EI Compendex database!

Contents

Deep Foundations

1943–2023: 80 Years of Research and Practice for Pile Foundations	3
Alessandro Mandolini	
Stress Distribution of Pile Group on Jakarta Diluvium Clay Using 3D Finite Element Method	55
Stefanus Diaz Alvi, Stella Liviana, and Paulus P. Rahardjo	
FEM Simulation of Single Pile Load Tests	69
Long Duc Phung	
The Effects of Ground Anchor Prestressing on Pile Group Reaction Force Redistribution and Settlement as Permanent Foundation of High-Rise Building Using 3D FEM	79
Stefanus Diaz Alvi, Yiska Vivian C. Wijaya, Bondan W. Anggoro, and Paulus P. Rahardjo	
Numerical Study on Behaviors of Vertically-Loaded Tender Net Foundations Supported by Piles	89
Han Vo-Cong, Kinji Takeuchi, Yasuo Tomono, and Tatsunori Matsumoto	
An Appraisal of the Second-Order Pile Buckling Model According to the 2nd Generation Eurocode 7	105
Gary Axelsson and Fredrik Jansson	
Study on Uplift Capacity of Belled Pile in Sandy Soil	119
Toru Watanabe, Kentaro Hama, Yoshihiro Horii, and Yoshitaka Nakanishi	
Some Experiences with Drilled Shaft Construction in Punjab Alluvium, Using Different Drilling Methods	135
Sadaf Saeed and Sohail Kibria	

Modified β-method for Pile Design in Partially Saturated Soils: Theoretical Considerations for an Effective Stress Framework	151
T. Matthew Evans, Josiah Baker, and Tuyen Ngoc Tran	
Axial Load-Bearing Capacity Solutions of PHC Nodular Pile: A New Advancement in Vietnam Engineering Practice	167
Tuetakoun Aphisith, Duy-Khuong Ly, Tan Nguyen, and Jim Shiau	
Bearing Characteristics of Sheet Piles Subjected to Vertical Monotonic and Quasi-Static Cyclic Load in Saturated Clay Ground	177
Xi Xiong, Jiapeng Yu, Lua Thi Hoang, and Tatsunori Matsumoto	
Enhancing Rapid Construction Profitability of the Monolithic Steel Structure of Pile–Pier for Bridges in Vietnam	191
Hanh Quang Le, Trinh Thi Tuyet Nguyen, and Masaya Higashi	
Design Challenges of Large Diameter and Long Steel Pipe Pile in High Plasticity Clay at Patimban Port Development Project	203
Ryota Mizuno, Le Phuong Dong, Aditya Karya, and Thanh T. Nguyen	
The Use of Rapid Load Test as Alternative Load Test Method of Bored Piles	221
Poh Hai Ooi and Yong Ping Oh	
Building up a Dataset for Investigation of the Load Transfer Mechanism of Bored Piles from Case Histories in Vietnam	233
Phi Nguyen-Dinh, Tuetakoun Aphisith, Tan Nguyen, and Jim Shiau	
Load–Displacement Relations of a Driven Steel Pipe Piles from Static and Rapid Load Tests, and Empirical Formulas Based on SPT and CPT: A Case Study at Sashima Test Yard	245
Shihchun Lin, Koji Watanabe, Yutaro Naka, and Tatsunori Matsumoto	
Correlation Between SPT Indexes of Soils to Pressing Pile Load and Settlement of Concrete Piles: An Experimental Study in Bac Giang, Vietnam	261
Van Tai Tang, Tran Khoa Vu, Praveen M. Huded, and Thuy Lan Chi Nguyen	
Comparative Static and Rapid Load Tests on Steel Pipe Piles: A Case Study at Sashima Test Yard	275
Shihchun Lin, Koji Watanabe, Shuichi Kamei, and Tatsunori Matsumoto	
Bearing Capacity Assessment of the Instrumented Shaft Grouting Barrette Pile by Conventionally Static Loading Test	291
Trung Thanh Le, Lan Vu Hoang Bach, and Hai Minh Nguyen	

State of Practice—Dynamic Load Test Monitoring of Driven Piles in the United States	307
Thai Nguyen	
Case Study: Dynamic Load Testing of a Jointed Concrete Pile Project in Malaysia	323
Thai Nguyen	
Fundamental Study on Stress Evaluation of Pile Using Optical Fiber Sensors	341
Akihito Nakazato, Koji Watanabe, Takuya Ozama, and Daizo Yamashita	
Development of t-z and q-z Curves for Driven Piles and Bored Piles in Alluvial Clay Soil Based on Fiber Optic Instruments—A Case Study in Bekasi, Indonesia	353
Prieschila C. Tamsir, Ricky Setiawan, Bondan W. Anggoro, and Paulus P. Rahardjo	
Case History of Soil–Cement Piles with H-Shaped Steels and Vertical Loading Tests	369
Junji Hamada, Yuji Taya, Kiyoshi Yamashita, and Hidemi Ikeda	
In-Situ Full Scale Horizontal Load Test on Soil–Cement Composite Pile	381
Shohei Koga, Koji Watanabe, and Tadahisa Yamamoto	
Continuum Analytical Models for the Ultimate Limit State Design of Energy Piles	395
Chiara Iodice and George Anoyatis (Georgios Anogiatis)	
Case Study—Feasibility of Energy Piles in a Cooling-Dominated Climate in Mexico	411
Norma Patricia López-Acosta, David Francisco Barba-Galdámez, and Martin Arenas-Moreno	
Modulus Number and Reference Tangent Modulus of Clays in the Red River Delta	425
Tien Dung Nguyen, Cong Kien Nguyen, Sung Gyo Chung, and Bengt H. Fellenius	
Behavior of Soil Surface Due to a Laterally Loaded Pile Based on a 1G Model Test and PIV	439
Mizuki Odagiri, Takatoshi Kiriya, and Yoshiharu Asaka	
Forensic Investigation of Pile Damages Using Dynamic Load Test and Continuous Monitoring, Case Study in Palembang, Indonesia	451
Stefanus Diaz Alvi and Paulus P. Rahardjo	

Geotechnical Design of Onshore Wind Turbine Foundations: Some Applications and Lessons Learned in Vietnam	461
Duc-An Ho, Trung-Kien Nguyen, and Tien Dung Nguyen	
Analysing the Suitability of the American Petroleum Institute Filter Press Test for Polymer Support Fluids	477
Daniel McNamara, Brian Sheil, Stephan Jefferis, and Chris Barker	
Influence of the Pulling-Out of the Temporary Sheet Pile Wall on the Adjacent Pile Foundation in Clay	487
Ngoc Bao Nguyen, Tae-Sung Ha, Yung-Ho Park, and Dong-Ju Yoo	
Studying on Bending Resistance of Monolithic Steel Structure of Pile–Pier	501
Thi Tuyet Trinh Nguyen, Sayuri Kitaichi, Duy Lam Dao, and Nobuyuki Matsui	
Machine Learning-Aided Prediction of Pile Behaviour: The Role of Data Quality	515
Thanh T. Nguyen, Thien Q. Huynh, Hadi Khabbaz, and Khuong Le Nguyen	
Tunnelling and Underground Spaces	
Urban Tunnelling—The Challenges of Creating Underground Space in Historic Cities	529
Giulia M. B. Viggiani	
Ground Movements in Shield Tunnelling for MRT Orange Line in Bangkok	567
Ochok Duangsano, Kangwan Kandavorawong, Auttakit Asanprakit, and Pornkasem Jongpradist	
Evaluating Interaction Between Structural Supports and Sedimentary Rock for a Tunnel with Penstock at a Hydropower Plant in Laos	581
Thi Minh Giang Le and Quang Huy Le	
Estimating the Maximum Support Pressure When Shallow Tunnelling in Soft Soils in Hanoi and Ho Chi Minh City	597
Minh Ngan Vu and Wout Broere	
The Design of Mountainous and Sub-sea Tunnels as Climate Resilient Infrastructures Using the Norwegian Method of Tunnelling (NMT)	611
Rajinder Bhasin and Arnstein Aarset	

A 3D Finite Element Analysis and Field Monitoring of the Residual Displacement of the Existing TBM Tunnel After Underground Culvert Construction: A Case Study in Ho Chi Minh City	623
Hung Van Nguyen, Duc Dinh Nguyen, Tam Trong Nguyen, and Duong Thuy Le	
Successful Implementation of Earth Pressure Balance Shield for Hanoi Metro Line 3 Project	633
Jeremy Lee and Thorsten Tatzki	
On Preparation and Assembly of TBMs for Metro Line No. 3 Project in Hanoi	649
Hoang Phuong Luu, Quoc Tuan Trinh, Van Quang Nguyen, and Tien Dung Nguyen	
Trans-Tokyo Bay Highway (Submarine Auto-Route)	665
Yukitake Shioi	
Evaluation of Jet Grouting Design Parameters for TBM Launching and Arrival in Bangkok Soils	681
Allan Sharma Neaupane, Kuo Chieh Chao, Ricky K. N. Wong, and Ochok Duangsano	
Remanufacturing, Refurbishment and Rebuilt: A Review of Herrenknecht Remanufacturing Process and its Application on Tunnel Boring Machines in Asia-Pacific Region	697
Mai Ngoc Khang Cao	
Applying Buttress Wall to Reduce Displacement of a Deep Excavation Adjacent to the Ben Thanh-Suoi Tien Metro Tunnel	711
Nghia Trong Le, Kien Trung Nguyen, and Trung Minh Nguyen	
Polynomial Regression Analysis Method for Predicting Excavation-Induced Deformation in Shanghai Soft Soil	727
Hechen Zhou, Ruituo Wu, Xiaoqiang Gu, and Zhaohui Qin	
FEM Back-Analysis of a Deep Excavation in Hanoi, Vietnam	741
Tuan Van Nguyen, Nam Quang Tran, and Truong Xuan Dang	
Evaluation of Retaining Wall and Surrounding Ground Behavior in Soft Cohesive Soil by FEM Analysis	761
Hiroto Kumagai, Takao Kono, and Shou Nishiie	
Comparing Prestressed Wales System and Traditional Shoring System Method for a Deep Excavation Using Bored Pilling Wall in Ho Chi Minh City	775
Nghia Trong Le, Vien Ngoc Truong, and Kien Trung Nguyen	

Effect of Diaphragm Wall Stiffness for a Deep Excavation on Adjacent Tunnel Deformation	791
Nghia Trong Le, Kien Trung Nguyen, Son Ngoc Nguyen, and Trung Minh Nguyen	
Finite Element Analysis of Buttress Wall to Reduce Lateral Deformation of Deep Excavation Adjacent to Tunnels in HCMC	811
Van Qui Lai, Thai Trung Le, Thi Thanh Hai Truong, and Tran Anh Toan Le	
Investigation of the Effects of Seepage from Excavation Pit on Surrounding Environment and Numerical Simulation Study	827
Yonglai Zheng, Xubing Xu, and Ruizhi Li	
Numerical Analysis on the Performance of Anchored Diaphragm Walls for a Deep Excavation in Hanoi	843
Thanh Son Nguyen and Quoc Khanh Nguyen	
Python-Based Visualization and Characterization of Subsurface Profile for a Long-Distance Subway Alignment in Manila	855
Elaine Marie Z. Peña, Pham Huy Giao, Noppadol Phien-wej, and Roy Anthony C. Luna	
Detection of Cavities Beneath Concrete Structures Using Acoustic Wave in Dry and Saturated Soils	873
Seonghun Kang, WooJin Han, Dongsoo Lee, and Jong-Sub Lee	
Automatic Detection Model for Underground Pipelines Using FDTD Analysis and Convolution Neural Network	881
Sang Yun Lee, Ki-il Song, Weiwei Zhang, and Joo Yeol Bae	
Assessing the Strength and Failure Mechanism of Cement-Filled Metamorphic Rock	893
Hoang-Khanh Le, Meng-Chia Weng, and Thi Kim Thoa Ho	
Laboratory Testing of Open-Dug Caisson Skin Friction During Sinking in Sands	905
Alexander W. Swallow, Jack O. Templeman, Bryn M. Phillips, and Brian B. Sheil	
Ground Deformation During the Construction of a Shield Tunnel in Sand and Gravel Layers	919
Chuanjin Ding, Jun Kuang, Xuedong Li, and Qiang Tang	
Ground Improvement	
Applications of Deep Vertical Vibratory Compaction	937
K. Rainer Massarsch	

Undrained Shear Strength Increase of Clay Among SCPs Examined in the Triaxial Cell	975
Yoichi Watabe, Aika Ohno, and Tomoka Togiya	
Numerical Analysis on Deformation of Soft Organic Soil Improved and Stabilized by Sand Columns	985
Viet Hung Le and Frank Rackwitz	
Comparison Between 3D FEM Analysis with Static Load Test Data of Downhole Dynamic Compaction: A Case Study of Ground Improvement Works on Volcanic Soils, East Java, Indonesia	997
Ahmad Kemal Arsyad, Martin Wijaya, and Paulus P. Rahardjo	
Behavior of Encased Stone Column-Reinforced Soil Under Eccentrically Inclined Loads	1011
Ashutosh Kumar Singh, Venkata Balaiah Kami, and Anumita Mishra	
Fundamental Study on Application of Artificial Neural Network Model to the Mixture Design of Soil Treated with Paper Sludge Ash-Based Stabilizer	1025
Phuon-Anh T. To, Kimitoshi Hayano, and Yoshitoshi Mochizuki	
Evaluation of Reinforcement of a Pile by Cement-Mixed Soil Improvement Using Model Tests and 3D Elasto-Plastic FEM Simulation	1035
Saya Okabe, Toshiyuki Kamata, Atsushi Shimamura, and Akihiko Wakai	
Strength and Verticality of Nordic Dry Deep Mixing Columns—A Case Study in Norway	1051
Solve Hov, Markus Nikolai Berner, Sigbjørn Rønning, and Bjørn Kristian Fiskvik Bache	
An Experimental Study on Vietnam's Circulating Resources Including Fly Ash for Soil Mixing Method	1067
Jae Hyun Park, Kwang Wu Lee, Wan Kyu Yoo, and Se Gwan Seo	
Effectiveness of Reclamation Technology by Combining Cement Deep Mixing Method (CDM) and Cement Pipe Mixing Method (CPM) on Patimban Port Development Project in Indonesia	1079
Tatsuru Aoyama, Yoshimitsu Yamada, Aditya Karya, and Hiromi Namiki	
Tailing Storage Facilities with Cemented Berms for Sustainable Production of Raw Materials	1099
António Viana da Fonseca, Isabela Caetano, Bernardo Meneses, and Sara Rios	

A Study of the Anisotropy of Improved Clay Using the Nordic Dry Deep Mixing Method	1113
Solve Hov, Priscilla Paniagua, and Kjell Karlsrud	
Effects of Cement Ratio and Curing Period on Interface Shear Strength of Cement-Treated Soil	1125
Thanh-Tu Nguyen and Minh-Duc Nguyen	
Construction Challenges and Quality Control and Assurance of Wet Deep Soil Mixing for an Approach Embankment of an Overbridge	1139
Kim Chan	
Mixture Design of Liquefied and Stabilized Soil Using High-Water-Content Cohesive Soil as Raw Material and Consistency of Quality in On-site Manufacturing	1157
Akihiko Izumi	
Assessment of Strength and Compaction Properties of Clays Treated with Paper Sludge-Based Stabilizers from Laboratory Mixture Tests	1171
Navila Tabassum, Kimitoshi Hayano, and Hiromoto Yamauchi	
California Bearing Ratio of Lateritic Soil Stabilized with Cement and Lime Mixtures	1185
Charles Nwaiwu and Everistus Arinze	
Improvement of Erosion Site Soils at Low Cement Content	1195
Charles Nwaiwu	
Reliability Analysis of Strength of Stabilised Soil	1209
Ansu Thomas	
Geotechnical Investigation and Evaluation of Steel Slag Mixed Ground	1217
Kosei Kawata, Kazuhiro Tsurugasaki, and Tomoya Sato	
Effective Soil Stabilization Solution for Windfarm Development in Southern Vietnam	1235
Viet Chanh Pham, Huy Dong Ngo, and Joe Jiunn Lau	
Preliminary Evaluation of the Viability of Single-Use Face Masks as a Substitute Nonwoven Geotextile	1251
Ella Jotojot, Donn Caryl Cabase, Marvin Lester Chu, and Ryan Ramirez	
The Use of Innovative Geocomposite Drainage System—Draintube to Achieve Optimal Drainage Efficiency at Pantai Nyanyi, Bali, Indonesia	1265
Saikat Chatterjee and Rocky Leroy	

Design of Ultimate Resistance of Geogrid-Reinforced Working Platforms for Tracked Plant Over Cohesive Subgrade	1273
Klomp maker Jörg, Vollmert Lars, and Nguyen Ngoc Hoang	
Effects of Sand Cushion with Geotextile Reinforcement on Improving Consolidation Behavior of Soft Clay	1285
Minh-Duc Nguyen, Thanh-Tu Nguyen, Van-Hiep Nguyen, and Hoang-Tuan Nguyen	
Vertical Drain Method for Expansion of Acceptable Capacity of Disposal Pond for Dredged Clay and Its Evaluation	1297
Masaaki Katagiri, Haruo Mori, Masahiro Kitahara, and Tomoyuki Nishino	
Design of Sand Moving Operation: Back Analysis and Settlement Prediction	1311
Nguyen T. Chi, Vo M. Thang, Vu A. Quan, and Truong T. Quy	
Evaluation of Instrumented Preloading with PVD in Deep Soft Bandung Lacustrine Soil	1325
Mikael Rafael, Stefanus Diaz Alvi, and Paulus P. Rahardjo	
Centrifugal Model Tests on Soil Behavior During Preload Removal from Ground Improved with Vertical Drains	1347
Daisuke Niina and Yoichi Watabe	
Impact of Microbial Metabolic Products on the Cone Penetration and Liquefaction Resistance of Sand	1361
Saswati Datta and Debasis Roy	
The Effects of RHA Dosage on Compressibility and Microstructural Development of Stabilized Calcite-Rich River Sludge	1375
Md Yachin Islam, Alex Otieno Owino, Abd Elmageed Atef, and Zakaria Hossain	
Using Enzyme-Induced Calcite Precipitation (EICP) to Improve Strength of Sandy Soils	1393
Mohsin Usman Qureshi, Azad Alshibli, Umayma Alshibli, and Ghassan Alkindi	
Dynamic Behavior and Undrained Shear Characteristics of Biomass Mixed Soil	1401
Tatsuya Yoshizaki, Taichi Hyodo, Naoki Tatta, and Shinya Uchida	
Design and Lesson-Learnt of the Eco-Friendly Bamboo Pile Foundation in Soft Soil—A Case Study in Patimban Deep Seaport	1413
Le Phuong Dong, Ryota Mizuno, Wahyu Trihadi, and Thanh T. Nguyen	

Strength and Deformation Characteristics of Soft Ground Stabilized by Bamboo Piles and Bamboo Mats	1431
Akio Takada, Masato Wada, Yuki Odagiri, and Kazuhiro Tsurugasaki	
The Characteristics of Soft Clay for Ground Improvement Distributed at Patimban Port Development Area in Indonesia	1445
Yoshimitsu Yamada, Tatsuru Aoyama, Ryota Mizuno, and Aditya Karya	
Liquefaction and Undrained Cyclic Behaviour in Fully and Partially Saturated Sands	1463
Fausto Molina-Gómez, António Viana da Fonseca, Cristiana Ferreira, and Bernardo Caicedo	
Sea Sand Used for Foundation Pit Backfill: A Case Study of Southern Breakwater for Large Ship Channel Route Entering Hau River, Vietnam	1475
Son Huu Nguyen, Vinh Trong Bui, and Tin Trung Huynh	
How to Recover Soil from Mixed Wastes? Separability of Soil and Wastes	1489
Atsushi Takai, Tomohiro Kato, and Takeshi Katsumi	
Deep Vibro Techniques' Performances and Carbon Emission Savings from Selected Industrial Projects in Vietnam	1503
William Chong, Cao Van Nghia, and Kam Weng Leong	
Effect of Fiber Material on Cyclic Behavior of Liquefied Stabilized Soil Under Cyclic Loading	1519
Hung Khac Le, Yukihiro Kohata, and Hung Quang Duong	
Applications of Big-Diameter Jet Grouting (BDJ) Method in Japan and Vietnam	1531
Tien Dung Nguyen, Hitoshi Oyama, Bao Hoang Nguyen, and Ngoc Phong Do	
Landslide and Erosion	
Prediction of the Hydraulic Gradient for Backward Erosion Piping in River Levees	1547
Mitsu Okamura	
On the Landslide Susceptibility and Resilience with Impact of Climate Change	1569
Keh-Jian Shou, Vi-Chi Lai, and Wei-Jeng Lin	
Spatially Distributed Mapping of Soil Erosion in a Debris Catchment After the 2018 Palu Earthquake	1579
I. Gede Tunas and Sriyati Ramadhani	

Large Slope Disaster at Hakusan District in Japan and Estimation of Risk by Rockfall	1591
Hiroshi Masuya, Takanari Fuji, and Yusuke Kurihashi	
Mechanism of Large-Scale Landslide Development and Remedial Methods—A Case Study in Vietnam	1607
Nguyen Duc Manh, Vu Tien Thanh, Ho Sy An, and Vo Minh Khoa	
A Case Study of Volcanic Soil Embankment Failure Triggered by Soil Softening Due to Water Infiltration and Water Seepage in Bandar Lampung, Indonesia	1619
Albert Johan, Andy Sugianto, and Paulus P. Rahardjo	
Rock Planar Slide—A Case Study at Tien Yen–Mong Cai Expressway, Vietnam	1637
Tuan-Nghia Do, Lan Chau Nguyen, Nguyen Quang Tuan, and Trang Thi Ha Vu	
Rehabilitation and Protection of Bridge Against Landslides: Case Histories at Semarang Ungaran Bridge	1651
Paulus P. Rahardjo, Muhrozi, and Y. Wisanto	
Mechanism and Rectification Method on Difficult Tomo Landslide, Sumedang, West Java, Indonesia	1665
Kirana Rongsadi, Albert Johan, Bondan W. Anggoro, and Paulus P. Rahardjo	
Stability Analysis and Parameter Sensitivity Analysis of Slopes Under Rainfall Infiltration Conditions	1685
Kaijie Wang, Chao Ge, Zongsizhe Chen, and Qiang Tang	
The Influence of K_0 Value on Excavated Slope Stability: Case Study Cisumdawu Toll Road, Indonesia	1699
Delaneira Princess Seourin, Martin Wijaya, Bondan W. Anggoro, and Paulus P. Rahardjo	
Finite Element Simulation for Creep Behavior Actualized Before the Landslide Due to Groundwater Fluctuations Based on Centrifuge Model Test	1711
Yuanying Li, Ryogo Isokawa, Shun Tateya, and Akihiko Wakai	
Effect of Wind Load According to Foundation Embedded Depth in Solar Power Plant in Slope	1727
Jong-Won Woo, Jeong-Yeon Yu, Jang-Hyun Park, and Ki-Il Song	
Application of TAG_FLOW Model for the Simulation of Slope Disaster in Central Vietnam Caused by a Typhoon in 2020	1737
Shota Fukushima, Nguyen Van Thang, Go Sato, and Akihiko Wakai	

Reinforcing a Collapsed Slope with a Combination of Complex Geotechnical Structures—A Case Study in Ha Long, Vietnam	1749
The Anh Pham, Viet Anh Pham, and Thiet Trung Le	
Research on Mechanical Characteristics of Plant Root Reinforced Slope Under Heavy Rainfall Conditions	1761
Zhibo Zhang, Jun Kuang, Xuedong Li, and Qiang Tang	
Effect of Horizontal Drain Installation Pattern on Drainage Performance and Slope Stability	1773
Mihira Lakruwan, Hiromu Oikawa, Akiyoshi Kamura, and Motoki Kazama	
Applicability of Corkscrew Extraction Technique in Strength Characterization of <i>Phragmites australis</i> Rooted Soil	1789
Abhijith Kamath, Karine van Bergen, Geert Ravenshorst, and Jan-Willem van de Kuilen	
Influences of Stress Ratio and Stress Path on Failure Behavior of Intact Completely Decomposed Granite	1801
Duc-Tung Bui and Cong-Oanh Nguyen	
Use of Electrical Resistivity Tomography for Detecting Quick Clay in Norway	1815
Thi Minh Hue Le, Saman Tavakoli, Jean-Sebastien L'Heureux, and Iason Papaioannou	
Soil–Water Characteristic Curve Analysis of Weathered Granite Soil According to Fine Content	1829
Sangbeen Lee, Jeongyoun Lee, and Jongwon Jung	
Shear Properties and Post-shear Water Content Distribution of Clayey Soil Under Different Loading Conditions by Ring Shear Tests	1841
Kyoma Kusano and Motoyuki Suzuki	
A Study on the Shear Strength Characteristics of Granite-Weathered Soil Using a Ring Shear Apparatus	1861
Daewon Lee, Siwon Ryu, and Jongwon Jung	
Bayesian Hierarchical Model on Crushability of Pumice Particle Strength	1871
I Wayan Ariyana Basoka, Kiyonobu Kasama, Zentaro Furukawa, and Ahmad Rifa'i	
Biopotential Response of Plants on Irrigation, Wind, and Tensile Stimuli	1885
Rina Takeda, Kiyonobu Kasama, and Zentaro Furukawa	

Effect of Fine Particles Content on Earthquake-Induced Failure of Volcanic Embankments Subjected to Rainfall	1897
Trong Nam Nguyen, Shima Kawamura, Minh Hieu Dao, and Takumi Inaba	
Geotechnical Modelling and Monitoring	
Continuum and Discrete Modelling of Penetration Problems	1915
Antonio Gens, Lluís Monforte, Marcos Arroyo, and Matteo Oryem Ciantia	
Monitoring Strains and Temperatures in a Deep Excavation Base Slab Using Fibre-Optic Bragg Gratings	1967
Peter J. Hensman and Brian B. Sheil	
Distributed Optical Fibre-Based Pore Water Pressure Sensor for Early Warning of Geohazards	1983
Kusumi Anjana, Madhubhashitha Herath, Jayantha Epaarachchi, and Nadeej Priyankara	
Bridge Condition Survey of Critical Bridges in the Philippines	1995
Rowena Garcia, Luis Ariel Morillo, Patrick Adrian Selda, and John Alejandro Rivera	
Study on Real-Time Monitoring of an Actual Slope and Slope Stability Management Criteria	2009
Shota Yoshida, Xi Xiong, Tatsuro Nakai, and Saiji Fukada	
Measurement Results of Lateral Displacement of the Earth-Retaining Wall Using 3-Axis MEMS Inclinator	2025
Takao Kono, Toshiaki Sugawara, and Teruhiko Sugimoto	
Shallow Foundation Design Using Dynamic Cone Penetrometer and Taking into Account Liquefaction Aspect	2035
Tuan-Anh Luong, Miguel Angel Benz-Navarrete, Philippe Reiffsteck, and Fabien Szymkiewicz	
Development of a Digital Twin System for Retaining Walls	2049
Dong-Gun Lee, Ki-il Song, Kyung-Nam Kang, and Joon-Sang An	
Intelligent Framework for Finite Element Analysis with Machine Learning and Back-Analysis Capabilities for Geotechnical Engineering	2059
Chin Yau Pang, Marco Liang, Zhenya Yang, and Chia Weng Boon	
Sustainable Dike Adaptation Measures Using Finite Element Method and Optimization Algorithm NSGA-II	2077
Kacper Cerek, Elnaz Hadjiloo, and Jürgen Grabe	

Contaminant Migration in Construction and Demolition Waste Roadbeds Under Rainfall	2093
Deming Kan, Jun Zhou, Jun Yin, and Qiang Tang	
Numerical Study on the Seismic Behavior of Narrow Back-to-Back Geosynthetic Reinforced Soil Walls with Different Reinforcement Arrangements	2107
Ramyasri Rachamadugu and Amit Prashant	
Comparative Study on Settlement of EPS Road Embankments by Numerical Method	2119
Quoc-Bao Truong, Anh-Tuan Vu, Tatsunori Matsumoto, and Duc-Long Phung	
Seismic Evaluation and Retrofitting of Deficient Masonry Building Considering SSI Effects	2133
Lakshmi Latha, Samit Ray-Chaudhuri, and Prishati Raychowdhury	
Large-Displacement Numerical Analysis of Soil Failure Mechanism for Soil-Embedded Cylinder Interaction	2147
Kien Trung Nguyen	
Coupled Thermal–Hydraulic–Mechanical Fluid Simulation—An Innovative Tool for the Design of Grouting in Soils	2157
Conrad Boley, Yashar Forouzandeh, and Lisa Wilfing	
Undrained Bearing Capacity of Strip Footing on Clayey Soil Subjected to Combined Eccentric and Inclined Loads	2171
Quang Ngoc Pham, Satoru Ohtsuka, and Vinh Ngoc Pham	
Numerical Simulations of Pile Foundations Considering Small and Large Deformations	2185
Sascha Henke, Maliha Tasnim Tilat, and Philipp Wiesenthal	
Scattering of Seismic Rayleigh Waves by a Semi-circular Basin with Hysteresis Material Model	2201
Kien Trung Nguyen, Hoang The Thao, Trong Nghia Le, and Truong Son Bui	
Numerical Shear Band Strengthening with Contact Modelling for the Increase of Load Capacity of Geotechnical Structures	2215
Elnaz Hadjiloo and Jürgen Grabe	
Calculation of Pore Pressure Dissipated from a Clay Layer Due to Groundwater Extraction Using Physics-Informed Neural Network (PINN) with Reference to Land Subsidence Analysis	2229
P. H. Giao and D. H. Hien	

Sensitivity Analysis of Fine-Scale Parameters in Triaxial Tests of Soil Particles Based on Discrete Elements	2237
Yanling Lu, Jun Zhou, Jun Yin, and Qiang Tang	
Exploring the Mitigation Measures of Overhanging Antidip Slope by Centrifuge Tests and DEM Modeling	2249
Wen-Chao Huang, Pei-Syuan Wu, and Mei-Wen Chen	
Numerical Modeling of Pull-Out Experiments on Assembly of Aluminum Rods Using DEM	2265
Kohei Gohji, Motoyuki Suzuki, and Minato Goya	
A Study on Thermal–Mechanical Coupling Behavior of Foliated Metamorphic Rocks	2281
Minh-Triet Pham, Hoang-Khanh Le, Meng-Chia Weng, and Wei-Han Wu	
Sandstone Damage Characteristics Based on Triaxial Test and Discrete Element Numerical Simulation	2295
Xiaoxia Qin, Chao Ge, Zongsizhe Chen, and Qiang Tang	
Detection of Voids in Karstic Terrains with 3D Surface-Based Seismic Waveform Tomography	2309
Majid Mirzanejad and Khiem T. Tran	
Utilization of Geophysical Methods for Hazard Assessment and Risk Management for Various Projects in the Philippines	2319
Kate Trishia Papina, Arian John Fruto, Roy Anthony Luna, and Ramon Quebral	
Investigation of Buried Objects in the Ground by Borehole Radar Surveys	2331
Keiji Ishikawa, Keito Sakaida, Dyah Sri Utami, and Shinsuke Karasawa	
Denoising Ground Penetrating Radar Images Using Generative Adversarial Networks	2343
Ngoc Quy Hoang, Seonghun Kang, and Jong-Sub Lee	
Comparison of Reconstituted Normally Consolidated Kaolinite and Illite in CIU Triaxial Tests Showcasing the Influence of Pore Fluid’s Salinity	2351
Maximilian Schröder and Jürgen Grabe	
Creep Behavior for Bentonite–Sand Mixture in Unsaturated–Saturated Condition	2363
Tomoyoshi Nishimura	

Deformation Properties of Red River Sand in Cyclic Triaxial Tests	2375
Nam Hong Nguyen and Manh Van Pham	
Modelling Pre- and Post-localisation Responses in Partially Saturated Soils	2389
Dat G. Phan, Giang D. Nguyen, Ha H. Bui, and Terry Bennett	
Evaluation of Marine Clays' Strain Rate Dependency During the Unloading Process	2401
Zheng Fan and Yoichi Watabe	
Strength-Deformation Behavior of Sandy Soil with Different Structures: Layered Structure Versus Uniform Structure	2413
Satoshi Matsumura, Daiki Takano, and Cyrille Couture	
Use of SWC-050 for Measuring Soil–Water Characteristic Curves	2425
Thi Phuong An Tran, Delwyn G. Fredlund, and Tran Thanh Nhan	
Composite Materials for Soil Improvement Applied to Saturated Clays—Requirements for the Material Properties	2435
Conrad Boley and Paul Pratter	
Consolidation Analysis in Unsaturated Soils with Non-Darcian Flow	2441
Amit Singh and Manash Chakraborty	
Influence of Rainfall on the Stability of Filtered Tailings Slope with Waste Rock Inclusions	2453
Hung Le and Thomas Pabst	
The Simplified Approach for Estimating Liquefaction-Induced Settlement Incorporating Viscous Models and Subgrade Reaction	2465
Chih-Wei Lu, Minh-Tam Doan, Jing-Cai Jiang, and An-Jui Li	
A Simulation of Lightweight Deflectometer Operation to Investigate Influences of Its Design on Soil Modulus of Elasticity	2479
Tram H. Nguyen, Yunje Lee, Yoowon Lee, and Jaehun Ahn	
Prediction of Ground Surface Settlements Induced by Deep Excavation Using a Closed-Form Solution	2489
Thanh Son Nguyen, Suched Likitlersuang, Van Qui Lai, and Trung Nghia Phan	
Digitalization and BIM in Geotechnics—Opportunities and Challenges	2503
Conrad Boley and Lisa Wilfing	

Microstructural Studies of Technogenic Soils in Alluvial Massifs	2513
Alan Lolaev, Aleksandr Badoev, Aleksan Oganessian, and Ilya Tvauri	
Specific Energy as Indicator of Liquefaction in Dynamic Centrifuge Experiments	2527
Andrei Dobrisan and Stuart Kenneth Haigh	
Technical Solutions for Improving Soil at Yen My Reservoir, Vietnam	2539
Van Toan Tran and Thai Binh Le	
Role of Drying and Wetting Soil–Water Characteristic Curves and Unsaturated Permeabilities on Slope Stability at Almaty	2549
Aiym Amantay, Alfrendo Satyanaga, Sung-Woo Moon, and Jong Kim	
Application of Artificial Intelligence on the Uncertainty Quantification Behavior of Creep Rock and Reliability-Based Optimization Design of Deep Tunnel	2561
Duc Phi Do, Minh Ngoc Vu, Dashnor Hoxha, and Gilles Armand	
Offshore Wind Power	
Time-Dependent Axial Capacity of Piles Driven in Clays and Sands	2579
Richard J. Jardine	
MMALE Simulations of Vibro-Installation of Offshore Monopiles	2631
Lisa Berki, Daniel Aubram, and Frank Rackwitz	
FE Modelling of Monopiles in Sand Under Monotonic and Cyclic Lateral Loads	2643
Hung Manh Ho, Ilaria Del Brocco, Zheng Li, and Federico Pisanò	
Geotechnical Design of Offshore Monopiles: Enhancing Efficiency and Expanding Analytical Scope	2659
Rauan Saturin and Minh Anh Nguyen	
DEM Analysis on Soil Horizontal Support Mechanism of Monopile Subjected to Cyclic Lateral Loading	2673
Shogo Ishii, Hirokazu Akagi, and Rikito Hayashida	
Model Tests to Investigate the Influence of the Spread Angle on the Pull-Out Resistance of the Belled Pile	2689
Chinatsu Mitsuoka, Shun Nomura, Hitaki Inaba, and Kazuo Tani	
Numerical Investigation of the Pile Installation Process in Clay and Its Influence on the Long-Term Cyclic Lateral Response of Offshore Foundations	2699
Patrick Staubach, Jan Macháček, and Torsten Wichtmann	

Experimental Investigation on the Time Variation of the Relationship Between the Resistance at the End of Installation and the Vertical Capacity of Pressed-in Piles	2709
Yukihiro Ishihara, Stuart Haigh, and Junichi Koseki	
Numerical Analysis for Failure Envelopes of Shallow Suction Caisson Underwater	2723
Sangwook Kang, Phuong T. H. Nguyen, Donghyun Lee, and Jaehun Ahn	
Pullout Capacity of Suction Anchors via 1G Model Tests Assuming Liquefied Sandy Ground	2731
Ryosuke Komuro, Masayuki Tomita, Akiyoshi Kamura, and Motoki Kazama	
Effect of Scour Depth on Natural Frequency of Offshore Wind Turbine with Tripod Suction Bucket Foundation	2745
Kyeong-Sun Kim, Byong-Youn Hwang, Min-Ho Lee, and Sung-Ryul Kim	
Deformation Analysis of Laterally Loaded Bucket Foundation of Offshore Wind Turbines Using HSS Model	2759
Jiandong Xiao, Xiaoqiang Gu, Zhenhao Shi, and Yifeng Lin	
Experimental Investigation of Bucket Foundations Subjected to Vertical Pullout Loading in Sand	2775
Seongho Hong, Quang Thien Buu Nguyen, Woong-Jong Park, and Sung-Ryul Kim	
Bearing Capacity of Circular Footing on c-ϕ Slope	2789
Minh Nhat Tran, Tirawat Boonyatee, Anh Tuan Le, and Van Qui Lai	
Long-Term Lateral Cyclic Response of Shallow Onshore Wind Turbine Foundations Resting on Dense Sand	2799
Chisom Ifeobu, Christelle Abadie, and Stuart Haigh	
Dynamic Performance Analysis of a 15 MW Floating Offshore Wind Turbine in the Ninh Thuan Offshore Area, Vietnam	2813
Thanh Dam Pham, Hai Nam Nguyen, Thanh Huyen Nguyen, and Du Van Toan	
Geo-engineering for Floating Wind Turbines	2827
Alan Crowle	
Effect of Foundation Tip Shape on Penetration Mechanism Visualized by Transparent Model Ground	2847
Rikuto Fujikata, Shun Nomura, and Kazuo Tani	

The Competitive Advantage of Onshore Lidar: Lessons from the Offshore Wind Industry Applications	2859
Matt Smith and Euan Macdonald	
Numerical Investigation of Drag Embedment Anchor Model Reduction for FOWTs in Coarse and Fine-Grained Baltic Sea Soil	2871
Duy A. Dao and Konrad Dicke	
Seabed Morphological Characterization and Shallow Geohazards at Offshore Binh Thuan Wind Farm Sites, Southern Vietnam Shelf	2887
Bui Viet Dung, Pham Quy Ngoc, Doan Huy Hien, and Do Van Chanh	
Scour Protection with Geotextile Sand Containers on Foundation Structures of Offshore Wind Turbines	2895
Janne Kristin Pries and Hoang Nguyen Ngoc	
Assessing the Wind Energy Potential of Bach Ho Field Through High-Resolution Downscaling Approach	2907
Nga Thi Thanh Pham, Thang Van Vu, Anh Lam Nguyen, and Han Trong Bui	
Modeling of Scholte Wave for Offshore Seismic Survey	2919
Quoc Kinh Tran, Chih-Ping Lin, Ernian Pan, and Tsai-Jung Wu	
Field Trials of Suction-Assisted Installation of Circular Steel Pipe Cofferdam in Silty Sand	2937
Ju-Hyung Lee, Jae-Hyun Kim, and Jae-Hyun Park	
Evaluation of the Potential for Reusing Dredged Material for Beach Nourishment in Vietnam	2949
Dung Duc Le and Tung Thanh Tran	

Estimating the Maximum Support Pressure When Shallow Tunnelling in Soft Soils in Hanoi and Ho Chi Minh City



Minh Ngan Vu and Wout Broere

Abstract The growing economy and increasing urban population create a high demand for transportation infrastructure. When surface space becomes limited and costly, underground space becomes a crucial solution to create new infrastructure. The increasing number of tunneling projects in soft soil conditions poses challenges regarding the risks of instability during the tunneling process. The research paper presents a novel compact blowout model developed by Vu and Broere (Tunn Undergr Space Technol 138, 2023) and evaluates the maximum support pressure for two specific cases: Ho Chi Minh City (HCMC) Metro Line No.1 and Hanoi Metro Line No.3. Assessing the support pressures applied at the HCMC Metro Line No.1 site, combined with field observations on stability, results in recommendations for similar projects in Hanoi and HCMC.

Keywords Tunnelling · Soft soils · Support pressure · Metro line

1 Introduction

The demand for transportation infrastructure in urban areas is rapidly increasing due to the ongoing development of the economy and the ongoing increase in urban population. Already, more than half of the world's population lives in cities and the projected growth of the world population until 2100 by another 2.5 billion people is expected to be concentrated in urban areas, and primarily those in coastal areas. This creates challenges, as these growing cities need more space for living as well as infrastructure for transport and distribution of food, water and energy [6]. As surface

M. N. Vu (✉)

Hanoi University of Mining and Geology, Hanoi, Vietnam
e-mail: vuminhngan@humg.edu.vn

W. Broere

Delft University of Technology, Delft, The Netherlands
e-mail: w.broere@tudelft.nl

space is often limited, use of underground space becomes essential to keep cities liveable and functioning.

As such, there is an increase in tunnelling projects in challenging locations with soft soils, high water tables, and limited right of way or cover. Tunnelling in such conditions has to deal with the challenges of keeping the tunnelling process stable, to limit the surface deformations and subsequent effects on nearby existing buildings. Especially when tunnelling with shallow overburden, these risks have to be taken into account, and the consequences of face instabilities can become significant. The precise determination of allowable support pressures, applied at the tunnelling face and in the tail void, plays an important role in ensuring the stability of the tunnelling process and minimizing the unexpected settlements at the surface. In these challenging conditions with limited cover, often the margin between the minimum support pressure, to prevent face collapse, and the maximum support pressure to prevent blowout, becomes small and difficult to handle during actual tunnelling. Therefore, a more exact determination of these limits and the margin between them becomes important to determine the possible alignment for shallow tunnels.

In limit analysis, the maximum support pressure is typically determined by considering the upper boundary condition. Leca and Dormieux [7] conducted a limit analysis for passive failure using elliptic cones originating from the tunnel face, and their findings indicated that this method yields very high allowable maximum support pressure. Similarly, Mollon et al. [10] employed a similar approach and obtained comparable high support pressures when studying solid passive failure mechanisms. Li et al. [8] and Liu et al. (2021) also reported similar results using this method. However, it is worth noting that the theoretical maximum allowable support pressure, also known as blowout pressure, estimated using the upper boundary condition in limit analysis approaches, often exceeds what has been observed in real-world field conditions and experiments. Using numerical and analytical simulation methods, Verruijt and Booker (1998) developed a 2D stability analysis, incorporating blowout. Wong and Subrin [14] and Mollon et al. (2010, 2013) introduced models that combined numerical simulation with limit analysis, encompassing 3D failure mechanisms. These models demonstrated a satisfactory agreement between the limit analysis and numerical models. However, they still tended to yield higher estimates for allowable pressures compared with real-world field observations. In a study on passive failure, Liu et al. [9] conducted one of the few available model tests in the literature. Their findings indicated a more confined area of failure than what was predicted by conical limit analysis models. Similarly, Li et al. (2009) argued that, for blowout or passive failure, it is necessary to consider a partial face mechanism rather than a full face mechanism, as the latter tends to overestimate the resistance of the soil body.

Experimental investigations in blowout have been performed. Berthoz et al. [3] conducted a series of tests using a unique reduced-scale model of an Earth Pressure Balance (EPB) machine in stratified soils to investigate both face collapse and blowout phenomena. The recorded blowout pressures from these tests showed significant differences when compared with the calculated pressures derived from the limit analysis models proposed by Subrin and Wong [11] and Wong and Subrin [14].

Despite suggestions that blowouts occur more frequently, only a limited number of blowout cases have been reported in the literature for recent tunneling projects. However, there is a notable and well-documented case of blowout that took place during the Second Heinenoord Tunnel project in the Netherlands, as reported by Bezuijzen and Brassinga [4] and Broere [5].

The other popular method is limit equilibrium method for estimating the maximum support pressure when tunnelling with the studies of Balthaus [2], Broere [5], Vu et al. [12], and Vu and Broere [13]. Most of the limit equilibrium models are based on the equilibrium condition of support force from the TBM and the forces of the pushed upward soil mass above the tunnel.

This paper focuses on the state-of-the-art models for estimating the maximum allowable support pressures, both applied at the tunnelling face and the tail void [13] with limit equilibrium method and compares these with field observations.

A back analysis is performed using the predicted and measured support pressures for the HCMC Metro Line No.1 project. Combined with site observations this paper shows that lower support pressures should have been applied at the tunnelling face during boring in order to prevent the occurrence of a blowout. The allowable range of support pressures for the Hanoi Metro Line No.3 project is also calculated based on these models and recommendations for the upcoming tunnelling works are made.

2 State-of-the-Art Blowout Model for Estimating Maximum Support Pressure When Shallow Tunnelling in Soft Soils

A popular assumption in limit equilibrium models of blowout is that a soil volume acting as a rigid soil body above the TBM is pushed upward when blowout occurs. For instance, the model proposed by Balthaus (1991) assumes that the pushed-up soil volume has the shape of a truncated obelisk. Figure 1 shows the model proposed by Balthaus (1991).

The wedge soil body weight G can be estimated as follows:

$$G = \gamma C \left[AB + AC \cotan\left(45^\circ + \frac{\varphi}{2}\right) + BC \cotan\left(45^\circ + \frac{\varphi}{2}\right) + \frac{4}{3} C^2 \cotan^2\left(45^\circ + \frac{\varphi}{2}\right) \right]. \quad (1)$$

The total support force at the top of the tunnelling face can subsequently be estimated as follows:

$$P = A.B.s, \quad (2)$$

where s is the support pressure.

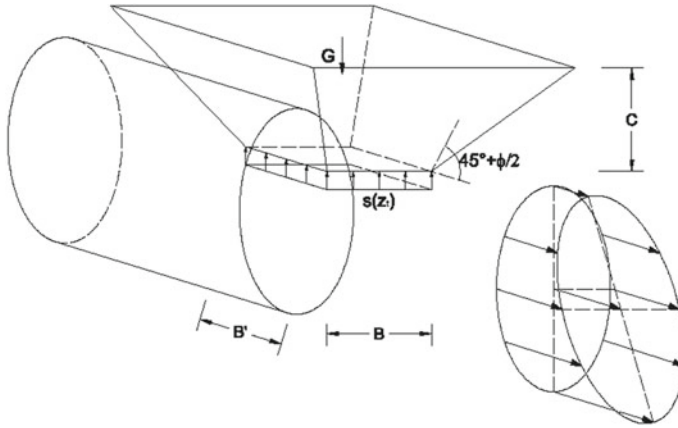


Fig. 1 Calculation model of Balthaus for the safety against blowout (Balthaus 1991)

After comparing the extent of the blowout soil volume in Balthaus (1991) to the results from numerical analysis of Soubra (2000), Li et al. (2009), Zhang et al. (Zhang et al. 2015), and experimental data in the study of Berthoz et al. [3], Vu and Broere [13] proposed a state-of-the-art model with a blowout volume that has been reduced, as can be seen in Fig. 2.

The dimensions A' and B' in this model are changed as follows:

$$A' = A + C \cotan\left(45^\circ + \frac{\varphi}{2}\right), \quad (3)$$

$$B' = B + C \cotan\left(45^\circ + \frac{\varphi}{2}\right). \quad (4)$$

Thus, the weight of soil body in Eq. (1) is then shown to be equal to:

$$G = \gamma C \left[AB + \frac{1}{2} BC \cotan\left(45^\circ + \frac{\varphi}{2}\right) + \frac{1}{2} AC \cotan\left(45^\circ + \frac{\varphi}{2}\right) + \frac{1}{3} C^2 \cotan^2\left(45^\circ + \frac{\varphi}{2}\right) \right]. \quad (5)$$

The actual effective support pressure length at the tunnel roof B is influenced by various factors such as the C/D ratio (depth to diameter ratio) of the tunnel, the encountered soil types, the type of support fluids employed, and the penetration mechanism of the support fluid. Determining this specific length of B in advance is challenging, as it relies on the complex interaction between the soil conditions and the support fluid applied during the tunnelling process. Similar to Balthaus (Balthaus 1991), the soil body's weight can be expressed as a function of the effective support pressure length at the tunnel roof B , using the following equation:

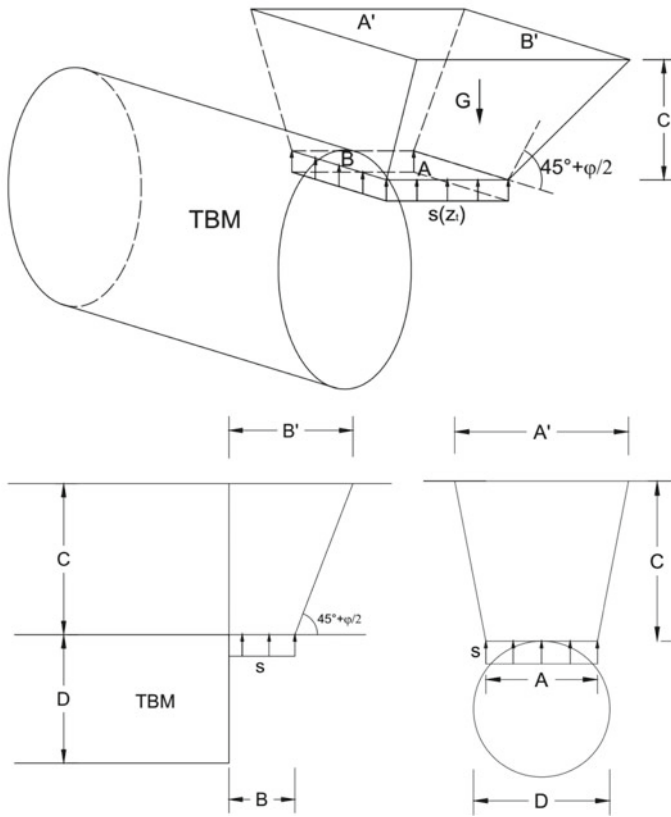


Fig. 2 Compact blowout model [13]

$$G = \alpha + \beta B. \quad (6)$$

The indexes α and β are determined as follows:

$$\alpha = \gamma C^2 \cotan\left(45^\circ + \frac{\varphi}{2}\right) \left[\frac{A}{2} + \frac{C}{3} \cotan\left(45^\circ + \frac{\varphi}{2}\right) \right], \quad (7)$$

$$\beta = \gamma C \left[A + \frac{1}{2} C \cotan\left(45^\circ + \frac{\varphi}{2}\right) \right], \quad (8)$$

and the maximum support pressure can be determined by establishing the equilibrium condition between the total support force P and the weight of the soil body G . Taking into account the safety factors, in accordance with Balthaus (1991), the maximum support pressure is given by:

$$\eta = \frac{\beta}{A.s} + \frac{\alpha}{A.B.s} > \eta_1 = \frac{\beta}{A.s} > \eta_2 = \frac{\gamma C}{s} \tag{9}$$

where η , η_1 , and η_2 are the safety factors. Here, safety factor η_1 is used in case of shallow and moderate tunnels. The value of $\eta_1 = 1.1$ as indicated in Vu and Broere [13].

The validation of this model with the results from three centrifuge tests in GeoDelft and five reduced scale experiments in Berthoz et al. [3] showed a good agreement.

3 Maximum Support Pressure Estimation for HCMC Metro Line No.1 Project

The first metro line in HCMC City, Vietnam, known as Metro Line No.1 HCMC from Ben Thanh to Suoi Tien Park, is a pilot railway system constructed in the city. This metro line has a length of 19.7 km and includes a 2.6 km underground section passing through densely populated areas such as Ba Son shipyard, the Saigon Municipal Opera House, and the Saigon River (Fig. 3). The soil composition along the tunnel route consists of soft soil, including layers of soft clay and silty sand.

The metro line alignment in HCMC city comprises fourteen stations, stretching from Ben Thanh station to Long Binh depot. Although the project for HCMC Metro Line No.1 was initiated in 2012, the underground construction was finally completed in 2020. The tunnel route passes beneath significant historical structures and densely populated areas, resulting in strict requirements for allowable settlements and deformations of existing surface buildings.

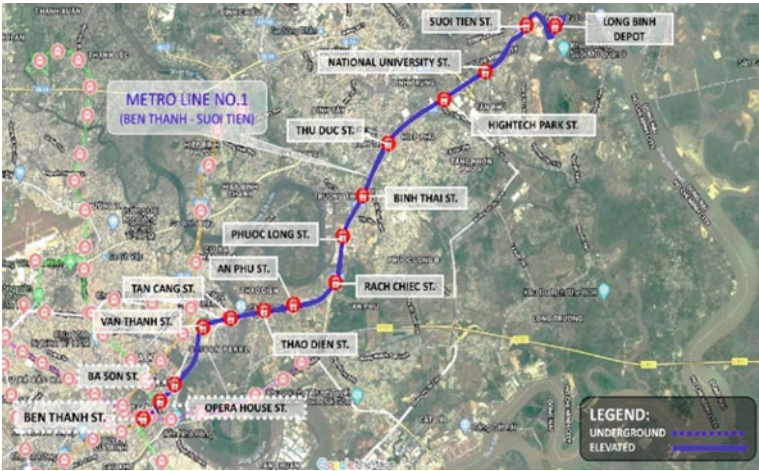


Fig. 3 HCMC metro line no.1 alignment in Vietnam

The tunnel segment has an outer diameter of 6.65 m and an inner diameter of 6.05 m. To minimize soil displacement in the surrounding area, an Earth Pressure Balance Tunnel Boring Machine (EPB TBM) was employed for two tunnel lines. These tunnels varied in depth from 11 to 30 m. The TBM used had a cutter head diameter of 6.82 m and a shield diameter of 6.79 m. The cutter head featured eight injection pipes, and the support pressures at the tunnelling face were regulated by an operator in the control room.

The geological conditions and soil parameters in HCMC Metro Line 1 outlined in Table 1 were utilized. The soil composition consists of three main soil types: a fill layer (F) at the top, alluvium layers, and diluvium materials at greater depths. Specifically, the fill layer is approximately 2 m thick, followed by alluvium layers reaching a depth of about 30 m. These alluvium layers comprise soft clayey silt (Ac2 and Ac3), silty fine sand layer 1 (As1), and sand layer 2 (As2). The diluvium layers mentioned in Table 1 consist of diluvium clayey silt (Dc) and a silty sand layer (Ds).

Figure 4 shows the designed tunnel alignment from the chainage Km 1 + 100 to Km 1 + 200. In this study, only the western line tunnel with shallow overburden is taken into account.

Figure 5 presents the analysis results of maximum support pressure from the chainage Km 1 + 100 to Km 1 + 200. A comparison to recorded support pressure at the site is also carried out. It can be seen that the site support pressures in this project tended to be larger than the predicted blowout pressures derived from the blowout model. This suggests that the operators of the Tunnel Boring Machine (TBM) had a tendency to operate it with a higher support pressure. The purpose behind this was to minimize excessive excavation of the soil in front of the TBM and enhance the stability of the tunnel face. However, this approach also posed a heightened risk of blowout occurrence. Furthermore, as depicted in the diagram, the measured blowout pressure does not correspond to the maximum applied support pressure during the excavation phase of tunnel construction. This can be attributed to the existence of additional structures like nearby buildings and road surfaces, which are not considered in the existing models due to the complexity of the calculations involved. Consequently, the true blowout pressure, accounting for the influence of surrounding structures, could potentially exceed the blowout pressure experienced in

Table 1 Soil parameters applied in HCMC metro line 1 project (based on UMRTL1-CP1b-TBMS-CGE-RPT-00073-C report)

No	Layer	γ (kN/m ³)	c (kPa)	φ (°)	K
1	F	19	0	28	0.6–0.5
2	Ac2	16.5	14	0	0.6–0.5
3	As1	19.5	0	31	0.6–0.5
4	As2	19.5	0	31	0.5
5	Dc	21	22	0	0.5

F Fill layer; *Ac* Alluvium Clay Layer; *As* Alluvium Sand Layer; *Dc* Hard Clay Silt γ Unit weight; c Cohesion; φ Friction angle; K Coefficient of lateral

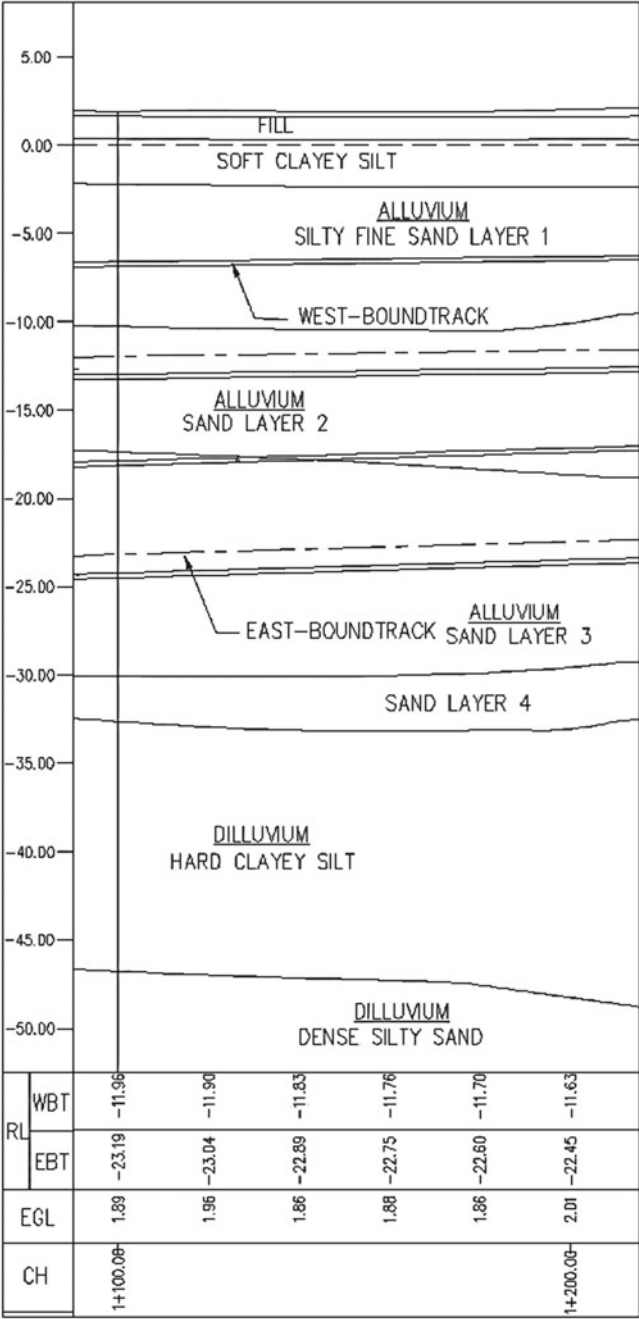


Fig. 4 Longitudinal geoprofile of metro line no.1 in HCMC city from the chainage Km 1 + 100 to Km 1 + 200

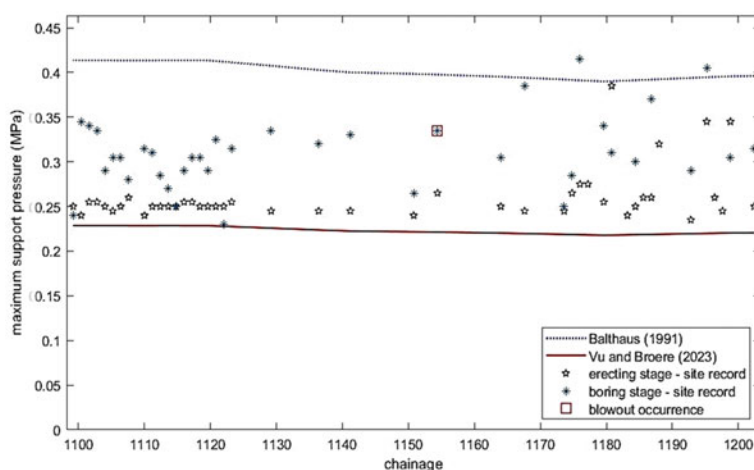


Fig. 5 Maximum support pressure estimation for HCMC Metro Line No.1 from the chainage Km 1 + 100 to Km 1 + 200

“greenfield” tunneling conditions. However, it is not advisable to incorporate these effects when estimating safe ranges for support pressure, particularly in urban areas.

A detailed analysis of the blowout occurrence at the chainage of Km 1 + 154.4 is shown in Fig. 6. It can be seen that the maximum support pressure derived from Balthaus’s model is larger than the recorded site value. The Vu and Broere model reveals a more appropriate blowout pressure, which remains conservative, estimated at approximately 70% of the recorded blowout pressure observed at the site. A numerical modeling of the tunneling process was carried out under “greenfield” conditions in Plaxis 3D. It was found that the tunneling operations indeed were expected to experience failure when a support pressure of 340 kPa was applied.

4 Maximum Support Pressure Estimation for Hanoi Metro Line No.3 Project

The Hanoi Metro Line No.3 is a part of the metro network in Hanoi, Vietnam. It constitutes the second line currently under construction and is anticipated to be finalized by 2024. Spanning a distance of 12.5 km, the line encompasses 12 stations running from Nhon terminal to Hanoi station. Figure 7 illustrates the line’s configuration, featuring an elevated section of 8.5 km and an underground section of 4 km.

Similar to the first metro line in Ho Chi Minh City, the underground portion of Hanoi Metro Line No.3 passes beneath densely populated areas, particularly from Kim Ma station to Hanoi station. Notably, it traverses underneath the Temple of Literature Van Mieu, a significant historical building in Hanoi. Due to the importance

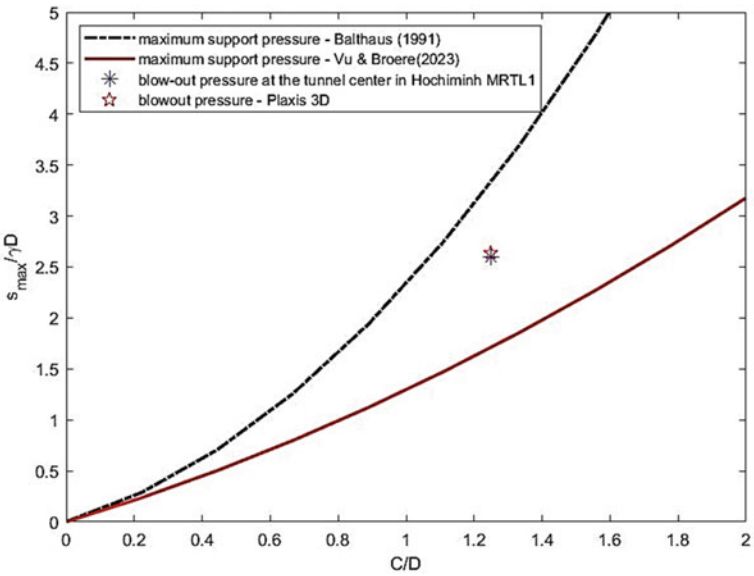


Fig. 6 Maximum support pressure estimation in blowout case in HCMC Metro Line No.1



Fig. 7 Hanoi metro line no. 3 alignment in Vietnam

of preserving nearby buildings, the tunnel construction adheres to strict settlement requirements to prevent any potential damage.

This study focuses on the underground segment between chainages Km 20 + 022 and Km 20 + 222. The geological composition of this specific segment is depicted in Fig. 8. It can be observed that the tunnel traverses beneath two to four layers of

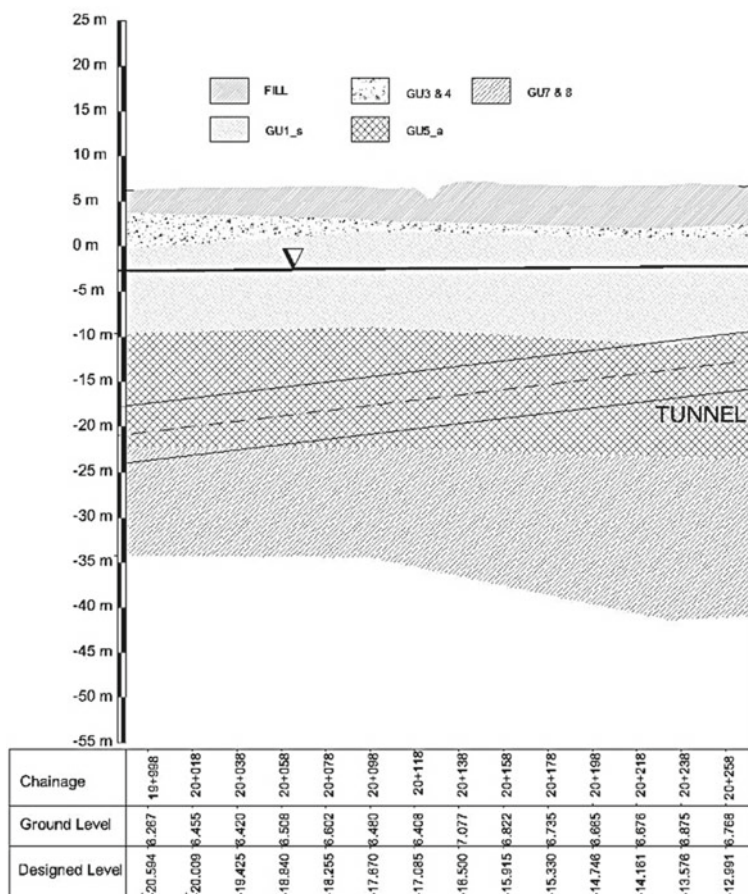


Fig. 8 Longitudinal geoprofile of Hanoi Metro Line No.3 from the chainage Km 20 + 022 to Km 20 + 222

soil in this section. The geotechnical properties of these four layers, namely the fill layer, GU1 layer (including GU3&4 layer) ranging in depth from 4 to 24 m, GU5 layer ranging in depth from 12 to 32 m below the surface, and GU7&8 layer ranging in depth from 26 to 45 m are provided in Table 2.

Figure 9 shows the predicted maximum support pressure applied to the tunnelling face from the chainage Km 20 + 022 to Km 20 + 222. It can be seen that the value of the maximum support pressure varies depending on the depth of the tunnel from about 600 kPa to 1000 kPa. With the depth of the tunnel from 25 to 30 m below the surface as can be seen in Fig. 8, the recommended support pressure that should be applied in tunnelling process in this section is from 450 to 600 kPa depending on the depth of the tunnel. Given the increased depth and cover compared with HCMC Metro Line No.1, these higher blowout pressures are expected and should allow for sufficient margin between the minimal support required and the maximum allowed pressure.

Table 2 Geotechnical properties of overburden soils of 200 m underground segment in Hanoi Metro Line No.3 project

Layer	γ (kN/m ³)	c (kPa)	φ (°)	K (–)
Fill	19	–	–	–
GU3&4	18.5	10	25	0.58
GU1s	16	5	20	0.66
GU5a	20	0	34	0.44
GU5b	20.5	0	35	0.43
GU7&8	21	0	40	0.36

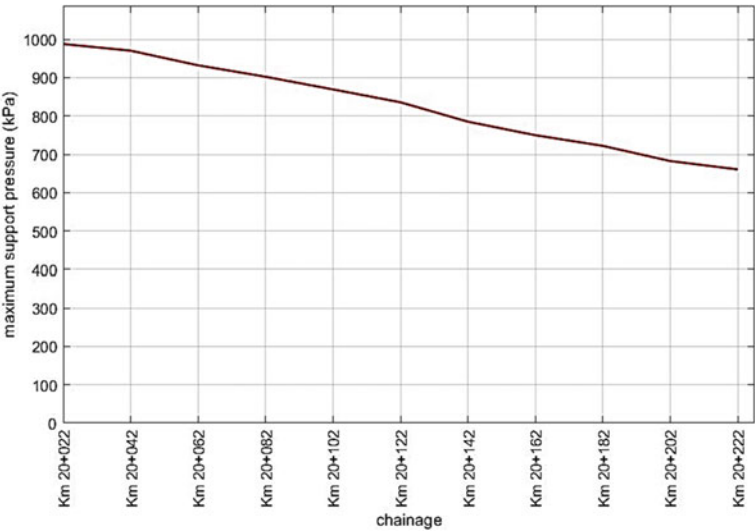


Fig. 9 Predicted maximum support pressures in Hanoi Metro Line No.3 from the chainage Km 20 + 022 to Km 20 + 222

5 Conclusions

The demand for urban transportation infrastructure is growing at a fast pace as the economy continuously develops and the urban population steadily rises. Since available surface area is restricted, underground space becomes crucial in order to maintain livable and operational cities. Consequently, the number of tunnel construction in soft soil conditions is on the rise. Particularly when tunneling with shallow depth, it becomes crucial to consider face instabilities risks. The paper uses a state-of-the-art compact blowout model developed by Vu and Broere [13] and assesses the maximum support pressure for two specific cases: HCMC Metro Line No.1 and Hanoi Metro Line No.3. The findings reveal that the support pressure exerted on the tunnel face in the HCMC Metro Line No.1 project of approximately 350 kPa was excessively high,

resulting in a blowout incident. For future projects, it is recommended to maintain a lower support pressure as a conservative limit, which in the case of the Hanoi Metro Line No.3 project, results in a recommended support pressure range from 450 to 600 kPa, depending on the tunnel's depth.

References

1. Anagnostou G, Kovári K (1994) The face stability of slurry-shield-driven tunnels. *Tunn Undergr Space Technol* 9(2):165–174
2. Balthaus H (1989) Tunnel face stability in slurry shield tunnelling. In: *Proceedings of 12th international conference soil mechanics and foundation engineering*, pp 775–778
3. Berthoz N, Branque D, Subrin D, Wong H, Humbert E (2012) Face failure in homogeneous and stratified soft ground: theoretical and experimental approaches on 1g EPBS reduced scale model. *Tunn Undergr Space Technol* 30:25–37
4. Bezuijen A, Brassinga HE (2006) Blow-out pressures measured in a centrifuge model and in the field. In: *Tunnelling: a decade of progress: GeoDelft 1995–2005*, pp 143–148
5. Broere W (2002) Tunnel face stability and new CPT applications
6. Broere W (2016) Urban underground space: Solving the problems of today's cities. *Tunn Undergr Space Technol* 55:245–248
7. Leca E, Dormieux L (1990) Upper and lower bound solutions for the face stability of shallow circular tunnels in frictional material. *Géotechnique* 40(4):581–606
8. Li D, Zhao L, Cheng X, Zuo S, Jiao K (2020) Upper-bound limit analysis of passive failure of a 3D shallow tunnel face under the bidirectional inclined ground surfaces. *Comput Geotech* 118:103310
9. Liu D, Liu X, Han Y, Xiong F, Liu R, Lin C, Demg Z, Xiao Y, Luo W (2022) Model test on the passive failure of slurry shield tunneling in circular-gravel stratum. *Earth Space Sci* 9(6):e2021EA002199
10. Mollon G, Dias D, Soubra AH (2011) Rotational failure mechanisms for the face stability analysis of tunnels driven by a pressurized shield. *Int J Numer Anal Meth Geomech* 35(12):1363–1388
11. Subrin D, Wong H (2002) Tunnel face stability in frictional material: a new 3D failure mechanism. *CR Mec* 330(7):513–519
12. Vu MN, Broere W, Bosch J (2015) The impact of shallow cover on stability when tunnelling in soft soils. *Tunn Undergr Space Technol* 50:507–515
13. Vu MN, Broere W (2023) A compact blowout model for shallow tunnelling in soft soils. *Tunn Undergr Space Technol* 138:105167
14. Wong H, Subrin D (2006) Stabilité frontale d'un tunnel: mécanisme 3D en forme de corne et influence de la profondeur. *Revue européenne de génie civil* 10(4):429–456